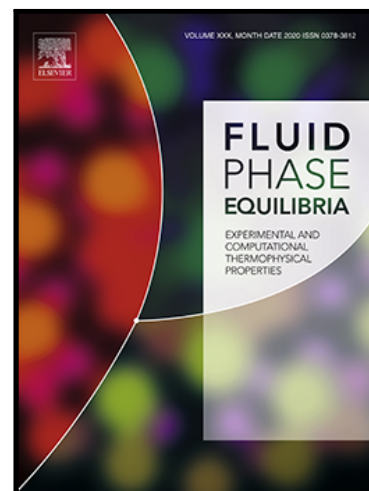


## Journal Pre-proof

Influence of excipients on solubility of oxcarbazepine: Modeling and prediction based on thermodynamic models

Qinxi Fan , Mingdong Zhang , Yewei Ding , Alexey I. Victorov , Yuanhui Ji

PII: S0378-3812(24)00226-7  
DOI: <https://doi.org/10.1016/j.fluid.2024.114251>  
Reference: FLUID 114251



To appear in: *Fluid Phase Equilibria*

Received date: 2 August 2024  
Revised date: 30 September 2024  
Accepted date: 8 October 2024

Please cite this article as: Qinxi Fan , Mingdong Zhang , Yewei Ding , Alexey I. Victorov , Yuanhui Ji , Influence of excipients on solubility of oxcarbazepine: Modeling and prediction based on thermodynamic models, *Fluid Phase Equilibria* (2024), doi: <https://doi.org/10.1016/j.fluid.2024.114251>

This is a PDF file of an article that has undergone enhancements after acceptance, such as the addition of a cover page and metadata, and formatting for readability, but it is not yet the definitive version of record. This version will undergo additional copyediting, typesetting and review before it is published in its final form, but we are providing this version to give early visibility of the article. Please note that, during the production process, errors may be discovered which could affect the content, and all legal disclaimers that apply to the journal pertain.

© 2024 Published by Elsevier B.V.

# Influence of excipients on solubility of oxcarbazepine: Modeling and prediction based on thermodynamic models

*Qinxi Fan<sup>1</sup>, Mingdong Zhang<sup>1</sup>, Yewei Ding<sup>1</sup>, Alexey I. Victorov<sup>2</sup>, Yuanhui Ji<sup>1</sup>, \**

<sup>1</sup>Jiangsu Province Hi-Tech Key Laboratory for Biomedical Research, School of Chemistry and Chemical Engineering, Southeast University, Nanjing, 211189, People's Republic of China.

<sup>2</sup>St. Petersburg State University, 7/9 Universitetskaya nab., 199034 St. Petersburg, Russia.

\*E-mail: yuanhui.ji@seu.edu.cn; yuanhuijinj@163.com

**ABSTRACT:** In this work, the solubility of oxcarbazepine in polymers (PEG 6000, PEG 20000, PVP K25, and PVP K30) and their aqueous solutions was investigated by experimental measurement and thermodynamic modeling. Firstly, the solubility of oxcarbazepine in water and polymers was modeled and the corresponding binary interaction parameters (oxcarbazepine/water and oxcarbazepine/polymer) were determined based on the experimental phase equilibrium data. Furthermore, the solubility of oxcarbazepine in the polymer aqueous solution (the mass ratios of polymers in water were 2%, 4%, and 6%) was predicted by the solid-liquid equilibrium (SLE) coupled with the Perturbed-Chain Statistical Associating Fluid Theory (PC-

SAFT). It was observed that the predicted results agreed well with the experimental data, and the average relative deviation (ARD) was less than 7%. In this study, the solubility of oxcarbazepine in polymer aqueous solution was successfully predicted through the SLE coupled with the PC-SAFT, which was expected to provide theoretical guidance for the selection of pharmaceutical excipients and the rational design of preparations.

**KEYWORDS:** Oxcarbazepine, Polymers, PC-SAFT, Solubility

## 1. Introduction

The poor solubility of active pharmaceutical ingredients (APIs) in water is one of the most difficult problems in the development of pharmaceutical engineering[1]. The biopharmaceutical classification system (BCS) classifies drugs according to solubility and permeability[2]: BCS Class I (highly soluble, highly permeable), BCS Class II (poorly soluble, highly permeable), BCS Class III (highly soluble, poorly permeable), BCS Class IV (poorly soluble, poorly permeable). An increasing number of potential APIs (40-70%) are classified as BCS Class II or IV[3], which are poorly soluble and face significant challenges in formulation and commercialization as oral dosage forms. Poorly soluble APIs cannot reach the minimum blood concentration at low doses but will cause greater toxic side effects at high doses[4]. That seriously limits their clinical application. In response to this challenge, many solubilization strategies have emerged. Common techniques for increasing the solubility of poorly soluble APIs include solid dispersions[5], salt-forming[6], eutectic[7], etc. Among these technologies, one factor that plays an important role in improving solubility and bioavailability is the addition

of excipients. How to select excipients suitable for specific APIs is a key step in pharmaceutical engineering[8, 9].

Currently, the Food and Drug Administration (FDA) has approved hundreds of excipients. Common excipients include sugars such as mannitol[10] and polymers such as polyethylene glycol (PEG)[11] and polyvinyl pyrrolidone (PVP), etc.[12] Because the mechanism of the influence of excipients on API solubility has not been fully studied, a large number of trial-and-error methods are still used to select the appropriate excipients[5, 13]. This is a tedious project, that often consumes a lot of manpower, material, and financial resources. With the help of a suitable theoretical model to describe and predict the solubility of APIs, the experimental workload can be reduced and the efficiency of formulation design can be improved.

The approach of chemical thermodynamics for solving the solubility problem is to employ molecular thermodynamic models. Common examples include the models based on the local composition concept: the non-random two-liquid (NRTL) model[5], the universal quasi-chemical model (UNIQUAC) model[14], and the Wilson model[15]. Gross and Sadowski proposed the PC-SAFT model that is based on the thermodynamic perturbation theory and has been widely used for electrolytes[16], polymers[17], and supercritical fluids[18]. The PC-SAFT model proved successful in establishing the relationship between the macroscopic properties of the fluid and the microscopic interaction parameters of molecules. In this model, the molecule is considered as a chain composed of hard spheres of the same size, and the attraction and repulsion within and between the molecules is described[19]. It is expected that the PC-SAFT model can

help accelerate the pharmaceutical engineering development process, and improve the screening efficiency and selectivity of excipients. It also reduces trial-and-error and time costs and improves preparation quality and safety.

In this paper, a neuropathic API, oxcarbazepine[20], used for localized and systemic seizures was selected as the model API; its molecular structure is shown in Fig. 1. Oxcarbazepine is a neutral lipophilic compound belonging to BSC Class II with low water solubility and high permeability[20]. PEG and PVP have been widely used to improve poorly soluble drugs due to their low toxicity, excellent hydrophilicity and biocompatibility[21, 22]. In this paper, four commonly used excipients PEG 20000, PEG 6000, PVP K30, and PVP K25 were selected as model excipients. Based on the experimental phase equilibrium data, the solubilities of oxcarbazepine in water and the polymers at different temperatures were modeled, and the corresponding binary interaction parameters were determined. The solubility of oxcarbazepine in different polymeric aqueous solutions (ternary systems) was predicted. This prediction does not rely on the solubility data of the ternary system and successfully predicts the solubility of oxcarbazepine in the ternary system through the SLE coupled with the PC-SAFT, which is expected to provide reliable theoretical guidance for the screening of pharmaceutical excipients.

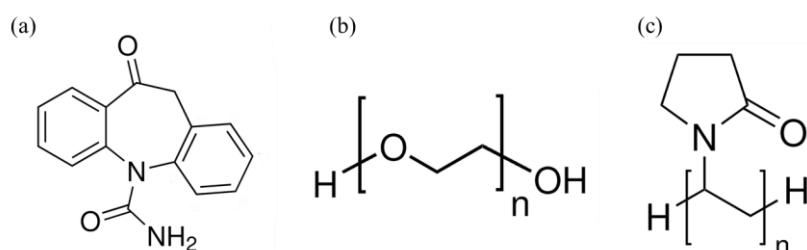


**Fig. 1.** Chemical structures of Oxcarbazepine (a), PEG (b), and PVP (c).

## 2. Theory

### 2.1 Solid-Liquid Equilibrium

In this study, excipients were considered as solvents and APIs as solutes. The solubility of the API in polymer excipients was determined using the SLE. The calculation formula is shown in Eq. (1), where the solubility is temperature-dependent[23].

$$x_{API}^L = \frac{1}{\gamma_{API}^L} \exp \left[ -\frac{\Delta h_{API}^{SL}}{RT} \left( 1 - \frac{T}{T_{API}^{SL}} \right) - \frac{\Delta C_{P,API}^{SL}}{R} \left( \ln \left( \frac{T_{API}^{SL}}{T} \right) - \frac{T_{API}^{SL}}{T} + 1 \right) \right] \quad (1)$$

Here  $x_{API}^L$  represents the solubility of the API in mole fraction,  $T_{API}^{SL}$ ,  $\Delta h_{API}^{SL}$  and  $\Delta C_{P,API}^{SL}$  represent the melting point in  $K$ , the enthalpy of melting in  $J/mol$ , and the difference of heat capacities in the solid and liquid phases of the API in  $J/mol/K$ , respectively.  $R$  and  $T$  represent the ideal gas constant in  $J/mol/K$  and temperature in  $K$ .  $\gamma_{API}^L$  is the activity coefficient of the API in the liquid phase, which is calculated by the PC-SAFT.

The weight fraction of the API in the API/polymer can be converted to the mole fraction follows Eq.(2).

$$x_{API}^L = \frac{C_{API}/M_{API}}{C_{API}/M_{API} + (1 - C_{API})/M_{polymer}} \quad (2)$$

Here  $C_{API}$  represents the solubility of the API in weight fraction,  $M_{API}$  and  $M_{polymer}$  represent the molar mass of the API and polymer in  $g/mol$ .

### 2.2. PC-SAFT

Based on statistical mechanics and Wertheim's first-order thermodynamic perturbation theory, the PC-SAFT model describes fluids that may contain chain-like

molecules[24]. In PC-SAFT, the residual Helmholtz energy ( $a^{res}$ ) is the sum of several contributions: the hard-chain contribution ( $a^{hc}$ ), the dispersive contribution ( $a^{disp}$ ) and the contribution caused by the association (hydrogen bonding) of the molecules ( $a^{assoc}$ ), as shown in Eq. (3).

$$a^{res} = a^{hc} + a^{disp} + a^{assoc} \quad (3)$$

The PC-SAFT model depicts the molecule as a chain of connected  $m_i^{seg}$  segments of diameter  $\sigma_i$ , using the hard sphere chain fluid as the reference fluid. In general, three pure component parameters are used to represent molecules: the number of segments ( $m_i^{seg}$ ), the diameter of segment ( $\sigma_i$ ) and the dispersion energy parameter ( $u_i/k_B$ ), where  $k_B$  is the Boltzmann constant. In associating fluids, to characterize the interaction between the donor and acceptor in the molecular hydrogen bond, the number of association sites ( $N_i^{assoc}$ ), the association volume parameter ( $k^{A_iB_i}$ ), and the association energy parameters ( $\varepsilon^{A_iB_i}/k_B$ ) are added. The Berthelot-Lorentz combining rule is used to describe the interaction between component  $i$  and component  $j$  in the mixture, as shown in Eqs. (4) and (5). To correct the dispersion energy parameter, the binary interaction parameter ( $k_{ij}$ ) is introduced [25], as shown in Eq. (6).

$$\sigma_{ij} = \frac{1}{2}(\sigma_i + \sigma_j) \quad (4)$$

$$u_{ij} = (1 - k_{ij})\sqrt{u_i u_j} \quad (5)$$

$$k_{ij} = k_{ij,T} \cdot T + k_{ij,0} \quad (6)$$

The Wolbach and Sandler mixing rules are used to describe the association energy ( $\varepsilon^{A_iB_j}$ ) and the association volume parameter ( $k^{A_iB_j}$ ) for the mixture[26], as shown in Eqs. (7) and (8).

$$\varepsilon^{A_i B_j} = 0.5 \times (\varepsilon^{A_i B_i} + \varepsilon^{A_j B_j}) \quad (7)$$

$$k^{A_i B_j} = \sqrt{k^{A_i B_i} k^{A_j B_j}} \times \left[ \frac{2 \times \sqrt{\sigma_{ii} \sigma_{jj}}}{\sigma_{ii} + \sigma_{jj}} \right]^3 \quad (8)$$

### 2.3 Determination of activity coefficients from PC-SAFT

The residual chemical potential ( $\mu_i^{res}$ ) is calculated from the residual Helmholtz energy ( $a^{res}$ , Eq. (2)), as shown in Eq. (9)[27].

$$\frac{\mu_i^{res}}{k_B T} = \frac{a^{res}}{k_B T} + Z - 1 + \frac{\partial(a^{res}/(k_B T))}{\partial x_i} - \sum_{j=1}^N x_j \left( \frac{\partial(a^{res}/(k_B T))}{\partial x_j} \right) \quad (9)$$

Here  $x_i$  and  $x_j$  are the mole fractions of components  $i$  and  $j$  in the fluid mixture, respectively, and  $Z$  is the compressibility factor, which can be obtained from Eq. (10).

$$Z = 1 + \rho(\partial(a^{res}/(k_B T))/\partial \rho) \quad (10)$$

Here  $\rho$  is the system density in  $kg/m^3$ .

The activity coefficient ( $\gamma_i^L$ ) can be obtained by the ratio of the fugacity coefficient of the component  $i$  in the mixture ( $\varphi_i^L$ ) to the fugacity coefficient of the pure liquid ( $\varphi_{0i}^L$ ), as shown in Eq. (11). Eq. (12) illustrates how to calculate the fugacity coefficient using the compressibility factor ( $Z$ ) and the residual chemical potential.

$$\gamma_i^L = \varphi_i^L / \varphi_{0i}^L \quad (11)$$

$$\ln(\varphi_i^L) = \mu_i^{res}/(k_B T) - \ln(Z) \quad (12)$$

The solubility of the API in solution is obtained by substituting the activity coefficient  $\gamma_i^L$  into Eq. (1) and solving the resulting nonlinear equation with respect to the mole fraction of API. The accuracy of the model is determined by root mean square deviation (RMSD) and mean relative deviation (ARD)[23], as shown in Eqs. (13) and (14).

$$ARD = \frac{1}{n_{exp}} \times \sum_{i=1}^{n_{exp}} \left| \frac{x_{exp,i} - x_{cal,i}}{x_{exp,i}} \right| \times 100\% \quad (13)$$



$$\text{RMSD} = \left[ \frac{1}{n_{exp}} \times \sum_{i=1}^{n_{exp}} (x_{exp,i} - x_{cal,i})^2 \right]^{0.5} \times 100\% \quad (14)$$

Here  $n_{exp}$  represents the number of data points used to calculate the error,  $x_{cal,i}$  and  $x_{exp,i}$  are the calculated and experimental solubilities, respectively, expressed in weight fraction.

### 3. Materials and methods

#### 3.1 Materials

Oxcarbazepine (purity > 98%) was purchased from Adamas Reagent Co. LTD (Shanghai, China). PEG 6000 and PEG 20000 were obtained from Energy Chemical Co., Ltd (Shanghai, China). PVP K25 and PVP K30 were bought from Macklin Co., Ltd (Shanghai, China). Fig.1 depicts the structures of various materials. All aqueous solutions were prepared with ultrapure water using an ultrapure water machine.

#### 3.2 Measurement of API solubility in excipients

DSC (Q20, TA, America) was used to determine the solubility of oxcarbazepine in polymers. In this study, based on the work of Tao et al.[28], a method for measuring the solubility of crystalline APIs in solvents was used to measure the solubility of APIs in polymers. Oxcarbazepine + polymer with a known oxcarbazepine content of  $x$  is heated gradually to a molten state. Assuming phase equilibrium is maintained during heating, the solubility of the oxcarbazepine in the polymer at the measured melting temperature is  $x$ . However, it is worth noting that the measured melting temperature is affected by the heating rate; The higher the heating rate, the higher the temperature obtained, and there is a linear correlation between the two[29]. Therefore, in the actual measurement,

the DSC heating rate is set to 15 K/min, 10 K/min, and 5 K/min. The result of different heating rates corresponding to different melting temperatures was extrapolated to a heating rate of 0 K/min, and the solubility of the oxcarbazepine in the polymer was obtained. In order to make the oxcarbazepine and the polymer fully mixed, weigh the corresponding quantities of the oxcarbazepine and the polymer, place them in a mortar, and fully grind them at room temperature. The mass fractions of oxcarbazepine were 0.85, 0.70, and 0.55, respectively.

### **3.3 Measurement of API solubility in excipients/water ternary systems**

The solubility of oxcarbazepine in polymer aqueous solution was determined by static method[23]. The mass fraction of polymers in water was 2%, 4%, and 6%, respectively. The aqueous solution of different mass fractions of the polymer was added to an excess amount of oxcarbazepine and placed in a 50 mL container. The temperatures selected in this experiment were 300.15 K, 305.15 K, 310.15 K, 315.15 K, and 320.15 K. To achieve thermodynamic equilibrium, the container was placed in a water-controlled thermostat and stirred with a magnetic stirrer for 72 hours and then keep it in static condition for 24 h until the solution became clear[30]. The samples were collected by syringe, filtered through a 0.45  $\mu\text{m}$  microporous membrane, and then measured. The concentration of oxcarbazepine was determined using the UV-vis spectroscopy (Analytic Jena Specord 210 Plus spectrophotometer, Jena, Germany). The UV absorption peak of oxcarbazepine is 254 nm, as shown in Fig 2 (a). The linear calibration curve for the absorbance versus concentration of oxcarbazepine in water was plotted and given in Fig 2 (b) ( $r^2 = 0.99685$ )

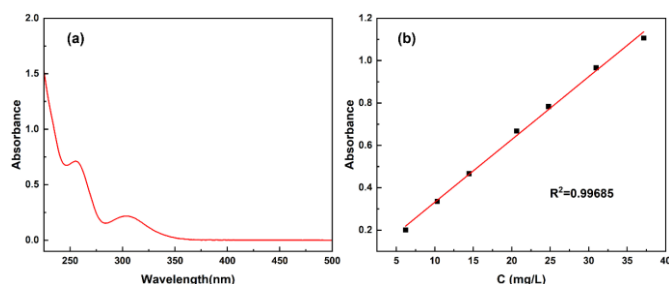


**Fig.2.** UV spectra of oxcarbazepine solubilized in water. (b) Absorbance vs. Concentration of oxcarbazepine drug at 254 nm.

## 4. Results and discussions

### 4.1 Solubility of oxcarbazepine in polymers

The solubility of oxcarbazepine in the polymer was determined by DSC. The melting temperatures of oxcarbazepine + polymer at heating rates of 15 K/min, 10 K/min, and 5 K/min were measured, and the melting temperatures at zero heating rates were calculated by a linear relationship. The linear equations between the melting temperature of oxcarbazepine + polymer and the DSC heating rate are shown in Table S1, and the DSC curves are shown in Fig. S1.

Fig. 3 shows the solubility of oxcarbazepine in the four polymers measured in the experiment. With the increase of polymer proportion, the melting temperature gradually decreases, which is more conducive to maintaining the stability of the drug. This is consistent with the research results of Khushboo Kothari et al[31]. They studied the effects of different polymer concentrations on the molecular mobility and physical stability of nifedipine solid dispersions and found that with the increase of polymer concentration, the molecular mobility of nifedipine solid dispersions decreased and the drug stability increased. Different polymers showed different solubility of oxcarbazepine at the same phase equilibrium temperature. As shown in Fig. 3, except

for the 85% PEG 20000 system, the ability of different polymers to enhance the solubility of oxcarbazepine follows the order: PEG 20000 > PEG 6000 > PVP K25 > PVP K30. In general, the solubilization effect of PEG on oxcarbazepine is stronger than that of PVP. This may be due to the stronger interaction of oxcarbazepine with hydroxyl groups in PEG than with amide groups in PVP.

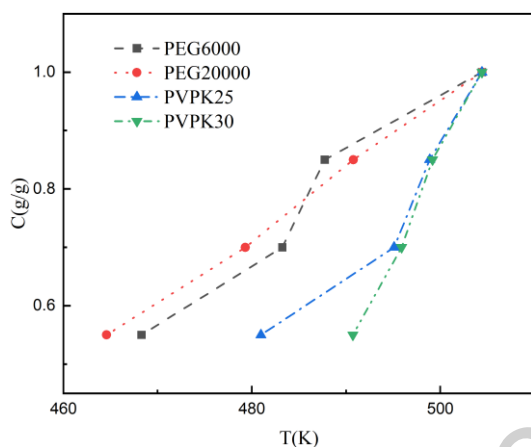


**Fig. 3.** Oxcarbazepine solubility in excipients (obtained by correlation between DSC heating rate and melting temperature): PEG 6000(dark gray squares), PEG 20000(red solid circles), PVP K25(blue solid triangles), PVP K30(green solid inverted triangles).

## 4.2 PC-SAFT parameters

### 4.2.1 Oxcarbazepine pure component parameters

PC-SAFT requires a small amount of experimental data to fit the parameters of the relevant substances. In general, the liquid density and vapor pressure of pure substances are often used to fit pure component parameters[32]. However, it is difficult to measure the density and vapor pressure of solid materials with high melting points and difficulty in volatilizing. For these substances, experimental data on the solubility in pure solvents can normally be used to determine the parameters[33].

In this study, the pure component parameters of oxcarbazepine were regressed from experimental data on the solubility in methanol, 1-propanol, 1-butanol, acetone, 2-propanol, ethanol, and acetonitrile. The solubility data were obtained from the literature[34]. The melting temperature, 504.42 K, and the melting enthalpy, 45.83  $kJ/mol$ , of oxcarbazepine are obtained from literature[20]. The pure component parameters of the four polymers PEG 6000, PEG 20000, PVP K25, and PVP K30 are obtained from literature and shown in Table 1.

**Table 1.** PC-SAFT pure component parameters of oxcarbazepine, excipients, and water.

	M (g/ mol)	$m_i^{seg}$	$\sigma_i$ (Å)	$\frac{u_i}{\kappa_B}$ (K)	$\frac{\epsilon^{A_i B_j}}{\kappa_B}$ (K)	$\kappa^{A_i B_i}$	$N_i^{assoc}$	Ref.
Oxcarbazepine	252.2	6.59	3.67	376.60	2522.8	0.02	1/1	this work
PEG 6000	6000	303.6	2.89	204.6	1799.8	0.02	2/2	[21]
			9					
PEG 20000	20000	1012	2.89	204.6	1799.8	0.02	2/2	[35]
			9					
PVP K25	25700	1045.	2.71	205.59	0	0.0450	231/23	[25]
		2				9	1	

PVP K30	58000	2360.	2.71	205.59	0	0.0451	521/52	[36]
		6					1	
Water	18.02	1.204	2.79	353.94	2425.7	0.0451	1/1	[37]
		7	3	5				

#### 4.2.2 Binary interaction parameter

Binary interaction parameters are used to correct the interaction between two components, which is particularly important for some strongly non-ideal systems, such as azeotrope systems and association systems[38]. In this study, binary interaction parameters are used to correct the dispersion energy parameters between components, which are temperature-dependent. The binary interaction parameters are fitted from the phase equilibrium data of the binary mixture, and the results are shown in Table 2. Among them, are the binary interaction parameters of PEG 6000, PEG 20000, PVP K25, and PVP K30 with water that were obtained from the literature. The binary interaction parameters of oxcarbazepine with PEG 6000, PEG 20000, PVP K25, and PVP K30 are obtained by fitting the solubility of oxcarbazepine in the polymers.

**Table 2.** PC-SAFT binary interaction parameter between different species.

system	$k_{ij,T}$	$k_{ij,0}$	Ref.
Oxcarbazepine + Water	$3.002 \times 10^{-4}$	-0.09636	this work
Oxcarbazepine + PEG 6000	$1 \times 10^{-4}$	-0.0756	this work
Oxcarbazepine + PEG 20000	$8.9 \times 10^{-5}$	-0.0526	this work
Oxcarbazepine + PVP K25	$1.2 \times 10^{-4}$	-0.046	this work
Oxcarbazepine + PVP K30	$1.05 \times 10^{-4}$	-0.037	this work
PEG 6000 + Water	$2.344 \times 10^{-4}$	-0.1035	[37]

PEG 20000 + Water	$2.344 \times 10^{-4}$	-0.1035	[35]
PVP K25 + Water	0	-0.1480	[37]
PVP K30 + Water	0	-0.1480	[36]

### 4.3 Modeling of oxcarbazepine solubility in binary systems

#### 4.3.1 Modeling of oxcarbazepine solubility in organic solvents and water

Based on the binary interaction parameters of oxcarbazepine with organic solvents and water and their pure component parameters, the solubility of oxcarbazepine in organic solvents and water can be modeled for different temperatures. As shown in Fig. 4 (a) and Fig.8, the solubility of oxcarbazepine in water and organic solvents increases with an increase of temperature, and the modeling results correlate accurately with the experimental data. The results of solubility modeling in organic solvents give  $ARD < 5\%$  and  $RMSD < 6 \times 10^{-5}$ , as shown in Fig. 4(b). The results of solubility modeling in water give  $ARD < 3\%$  and  $RMSD < 1 \times 10^{-5}$ , as shown in Fig. 8 (b).

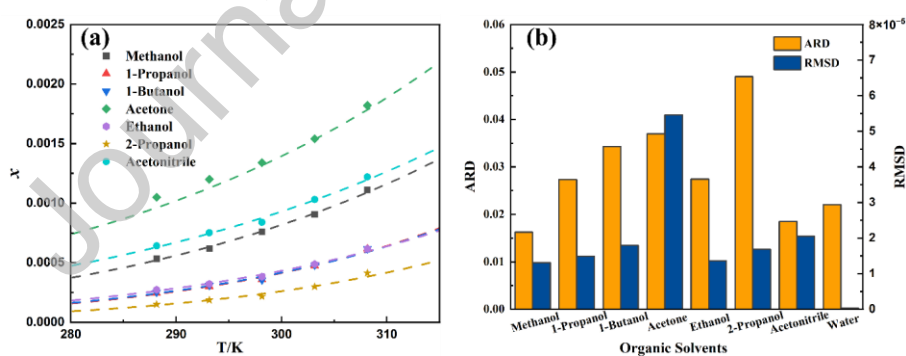


**Fig. 4.** (a) Solubilities of oxcarbazepine in different pure solvents: methanol (black solid squares), 1-propanol (red solid triangles), 1-butanol (blue solid inverted triangles), acetone (green solid diamonds), ethanol (purple solid hexagons), 2-propanol (yellow solid stars), acetonitrile (aqua green solid circles); Dashed lines are the modeled solubility with PC-SAFT. (b) ARD (orange) and RMSD (blue) between

the experimental and modeled oxcarbazine solubility in different pure solvents.

#### 4.3.2 Modeling of oxcarbazine solubility in polymers

In this study, the solubility-versus-temperature curve of oxcarbazine in polymers PEG 6000, PEG 20000, PVP K25, and PVP K30 shown in Fig. 5 was obtained using the binary interaction parameters of oxcarbazine with polymers and the pure component parameters of PC-SAFT. The black dots in this figure are experimental values, and the black solid lines are PC-SAFT modeling results. The model results are basically consistent with the experimental values. The ARD of oxcarbazine-polymer modeling is less than 12%, and the RMSD is less than 0.1, as shown in Fig. 6.

In Fig. 5, the region above the solubility curve is the thermodynamically stable region, and the drug is in an amorphous state when it is in this region. When the concentration of the drug in the preparation exceeds the solubility, the amorphous drug will recrystallize. The size of the area above the curve shows the ability of the polymer to maintain the thermodynamic stability of the drug, and the larger the area, the stronger the ability to maintain the stability of the amorphous drug. As shown in Fig. 5, the area proportion of the thermodynamic stability zone increases in the order: PEG 20000 > PEG 6000 > PVP K25 > PVP K30.

In theory, the solubility curve can be used to measure the melting temperature by DSC. However, when the temperature is low and the glass transition temperature of the system is close, it is difficult for the system to reach thermodynamic equilibrium due to the high viscosity of the drug-polymer system, so only part of the curve can be obtained in the experiment, and the workload is huge[39]. In this study, the solubility curve of



oxcarbazepine in polymers was modeled by PC-SAFT based on a small amount of experimental data. This method saves a lot of manpower, material, and financial resources, and provides some guidance for the screening of excipients in pharmaceutical preparations.

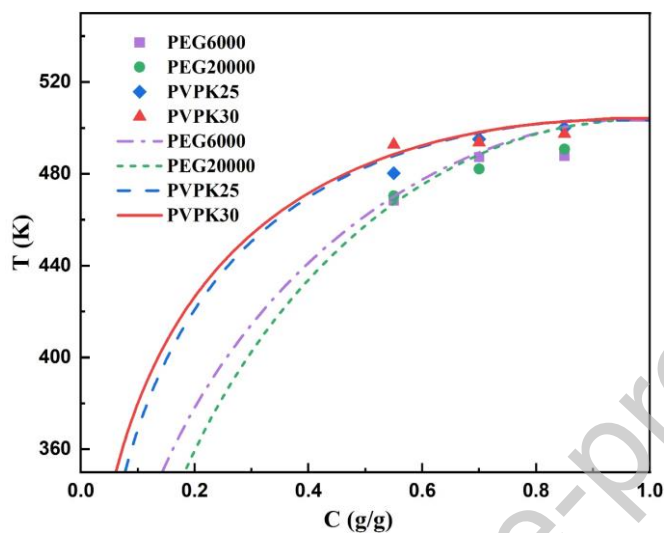


**Fig. 5.** Solubilities of oxcarbazepine in different polymers. Dots represent experimental measurements: PEG 6000(purple solid squares), PEG 20000(green solid circles), PVP K25(blue solid diamonds), PVP K30(red solid triangles) and the full, dashed, dot-dashed, short-dashed lines denote the modeled solubility with PC-SAFT: PEG 6000(purple dashed-dot line), PEG 20000(green short dashed line), PVP K25(blue dashed line), PVP K30 (red solid line).

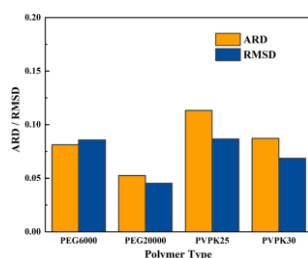


**Fig. 6.** ARD (orange) and RMSD (blue) between the experimental and modeled API solubility.

#### 4.4 Prediction of solubility of oxcarbazepine in ternary systems

The solubility of oxcarbazepine in PEG 6000, PEG 20000, PVP K25, and PVP K30 polymer aqueous solutions was predicted by the solid-liquid equilibrium combined with the PC-SAFT without relying on the solubility data for the ternary system. In part 4.2, the phase diagrams of oxcarbazepine + water, oxcarbazepine + polymer (PEG 6000, PEG 20000, PVP K25, PVP K30) binary systems are established, and the corresponding binary interaction parameters are obtained. The parameters of the binary interaction between polymer and water are obtained from the literature. The interaction parameters are summarized in Table 2. Using these parameters in the PC-SAFT model combined with the thermodynamic condition of solid-liquid equilibrium, we predicted the solubility of oxcarbazepine in the aqueous solutions of polymers by the Fortran programs within the Version 16.8.3 of Visual Studio Community 2019[24]. In order to verify the accuracy of the PC-SAFT model in predicting the solubility of oxcarbazepine in polymer aqueous solution in the ternary system, experiments were conducted according to part 3.3, and the results are shown in Table S2. The experimental results show that PC-SACT accurately predicts the solubility of oxcarbazepine in the polymer aqueous solution without relying on the experimental data in the ternary system. As shown in Table S2 and Fig.7, the ARD of the solubility prediction of oxcarbazepine in polymer aqueous solutions is less than 7%, and the RMSD is less than  $4 \times 10^{-6}$ .

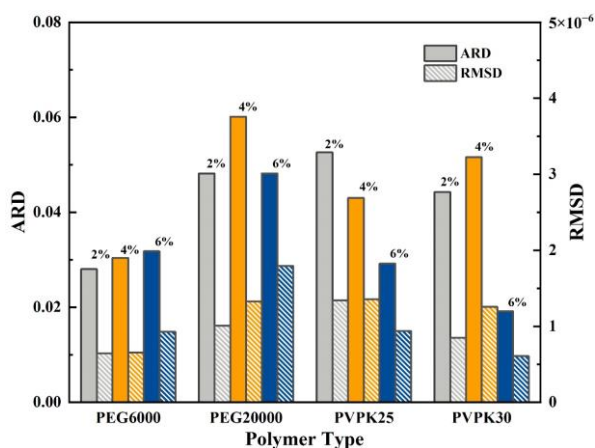


**Fig. 7.** ARD and RMSD between the experimental and predicted oxcarbazepine solubility in ternary systems. Gray, orange, and blue represent polymer solutions with a polymer mass fraction of 2%, 4%, and 6%, respectively. Bars without slashes represent ARD, and bars with slashes represent RMSD.

The prediction and experimental results of oxcarbazepine in four polymer aqueous solutions are shown in Fig. 8 and Table S2. The solubility of oxcarbazepine in polymer aqueous solution increases with the increase of temperature. Compared with the pure water system without polymer, the solubility of oxcarbazepine in the polymer-containing systems significantly increases. PEG 6000, PEG 20000, PVP K25, and PVP K30 showed good solubilization effects on oxcarbazepine. One reason for the increased solubility of oxcarbazepine in presence of the polymers can be attributed to increased wettability and decreased interfacial tension. The polymers selected in this study were all hydrophilic carriers, which greatly improved the wettability of the hydrophobic surface of the poorly soluble drug oxcarbazepine in water[40]. The solubilizing effect of oxcarbazepine is different, depending on the type and mass fraction of the polymer. The solubility of oxcarbazepine in 2%-6%PEG aqueous solution is 1.4-2.3 times that

in pure water, and the solubility in 2%-6%PVP aqueous solution is 1.8-3.0 times that in pure water. The effect of PVP K25 and PVP K30 on improving the solubility of oxcarbazepine in the aqueous solution was significantly better than that of PEG 6000 and PEG 20000. This is inconsistent with the dissolution rule of oxcarbazepine in the polymer (anhydrous state) obtained in part 4.1. The reason may be that the addition of water affects the interaction between oxcarbazepine and polymer in the system. Consequently, the stronger solubilizing effect of PVP can be attributed to its higher potential of forming multiple hydrogen bonds with drug molecules compared to relatively weaker interactions of PEG. In the systems containing PEG, the solubilization effect of PEG 6000 on oxcarbazepine is obviously better than that of PEG 20000, which is consistent with the study of Paus et al[21]. With the increase of PEG molar mass, API solubility decreases. When the mass fraction of the polymer is increased, the solubilization effect is more significant. This can be attributed to the increased wettability and the higher proportion of functional groups that can interact with drug molecules as the polymer mass fraction increases.

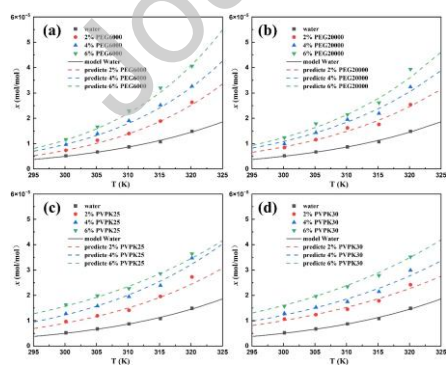


**Fig. 8.** (a) Solubility of oxcarbazepine in water (black solid squares), in water with 2 wt % PEG 6000 (red solid circles), in water with 4 wt % PEG 6000 (blue solid triangles), and in water with 6 wt % PEG 6000 (green solid inverted triangles);

(b) Solubility of oxcarbazepine in water (black solid squares), in water with 2 wt % PEG 20000 (red solid circles), in water with 4 wt % PEG 20000 (blue solid triangles), and in water with 6 wt % PEG 20000 (green solid inverted triangles); (c) Solubility of oxcarbazepine in water (black solid squares), in water with 2 wt % PVP K25 (red solid circles), in water with 4 wt % PVP K25 (blue solid triangles), and in water with 6 wt % PVP K25 (green solid inverted triangles); (d) Solubility of oxcarbazepine in water (black solid squares), in water with 2 wt % PVP K30 (red solid circles), in water with 4 wt % PVP K30 (blue solid triangles), and in water with 6 wt % PVP K30 (green solid inverted triangles). Dots are solubility values from experimental measurements. Solid black line, dashed red line, dashed blue line, and dashed green line represent the solubility of oxcarbazepine in water modeled by PC-SAFT, and the solubility predicted by PC-SAFT in aqueous polymer solution (polymer mass fraction: 2%, 4%, 6%, respectively).

## 5. Conclusions

In this work, thermodynamic condition of solid-liquid equilibrium and the PC-SAFT model were used to predict the solubility of oxcarbazepine in the aqueous solutions containing PEG 6000, PEG 20000, PVP K25, and PVP K30 without relying on the solubility data of ternary system. A high accuracy of these predictions has been verified experimentally. Firstly, based on the experimental phase equilibrium data, the solubility of oxcarbazepine in water and polymers was modeled and the corresponding binary interaction parameters were determined. Then, the solubility of oxcarbazepine in the polymer aqueous solution is predicted without relying on the solubility data of the

ternary system. The predicted results of the model agree well with the experimental data, and the average relative deviation is less than 7%. This indicates that the PC-SAFT has high accuracy and reliability in predicting the solubility of oxcarbazepine, which is expected to provide guidance for the screening of pharmaceutical excipients and important theoretical support for drug development in the pharmaceutical industry.

## 6. CRediT authorship contribution statement

**Qinxi Fan:** Experimental and theoretical investigation, Conceptualization, Writing – original draft, Writing – review & editing.

**Mingdong Zhang:** Methodology, Experimental and theoretical investigation, Writing – review & editing.

**Yewei Ding:** Software, Writing – review & editing.

**Alexey I. Victorov:** Supervision, Writing – review & editing.

**Yuanhui Ji:** Funding acquisition, Project administration, Resources, Conceptualization, Supervision, Writing – review & editing.

## 7. Declaration of Competing Interest

The authors declare that they have no known competing financial interests or personal relationships that could have appeared to influence the work reported in this paper.

## 8. Data availability

Data will be made available on request.

## 9. Acknowledgments

The authors gratefully acknowledge the financial support for this research from

the National Natural Science Foundation of China (grant nos. 22278070 and 21978047).

## REFERENCES

- [1] S. Halder, F. Ahmed, M. L. Shuma, M. A. K. Azad, E. R. Kabir. Impact of Drying on Dissolution Behavior of Carvedilol-Loaded Sustained Release Solid Dispersion: Development and Characterization [J]. *Heliyon*, 6(2020) e05026.<http://dx.doi.org/10.1016/j.heliyon.2020.e05026>
- [2] M. Lindenberg, S. Kopp, J. B. Dressman. Classification of Orally Administered Drugs on the World Health Organization Model List of Essential Medicines According to the Biopharmaceutics Classification System [J]. *Eur J Pharm Biopharm*, 58(2004) 265-278.<http://dx.doi.org/10.1016/j.ejpb.2004.03.001>
- [3] M. S. Poka, M. Milne, A. Wessels, M. Aucamp. Sugars and Polyols of Natural Origin as Carriers for Solubility and Dissolution Enhancement [J]. *Pharmaceutics*, 15(2023).<http://dx.doi.org/10.3390/pharmaceutics15112557>
- [4] X. Liu, L. Zhao, B. Wu, F. Chen. Improving Solubility of Poorly Water-Soluble Drugs by Protein-Based Strategy: A Review [J]. *Int J Pharm*, 634(2023) 122704.<http://dx.doi.org/10.1016/j.ijpharm.2023.122704>
- [5] R. Malkawi, W. I. Malkawi, Y. Al-Mahmoud, J. Tawalbeh. Current Trends on Solid Dispersions: Past, Present, and Future [J]. *Advances in Pharmacological and Pharmaceutical Sciences*, 2022(2022) 5916013.<http://dx.doi.org/10.1155/2022/5916013>
- [6] L. Liu, Q. An, Y. Zhang, W. Sun, J. Li, Y. Feng, Y. Geng, G. Cheng. Improving the Solubility, Hygroscopicity and Permeability of Enrofloxacin by Forming 1:2 Pharmaceutical Salt Cocrystal with Neutral and Anionic Co-Existing P-Nitrobenzoic Acid [J]. *J Drug Delivery Sci Technol*, 76(2022) 103732.<http://dx.doi.org/10.1016/j.jddst.2022.103732>
- [7] G. C. Bazzo, B. R. Pezzini, H. K. Stulzer. Eutectic Mixtures as an Approach to Enhance Solubility, Dissolution Rate and Oral Bioavailability of Poorly Water-Soluble Drugs [J]. *Int J Pharm*, 588(2020) 119741.<http://dx.doi.org/10.1016/j.ijpharm.2020.119741>
- [8] D. M. Walden, Y. Bunday, A. Jagarapu, V. Antontsev, K. Chakravarty, J. Varshney. Molecular Simulation and Statistical Learning Methods toward Predicting Drug-Polymer Amorphous Solid Dispersion Miscibility, Stability, and Formulation Design [J]. *Molecules*, 26(2021) 182.<http://dx.doi.org/10.3390/molecules26010182>
- [9] F. Yang, Y. Su, J. Small, C. Huang, G. E. Martin, A. M. Farrington, J. DiNunzio, C. D. Brown. Probing the Molecular-Level Interactions in an Active Pharmaceutical Ingredient (Api)-Polymer Dispersion and the Resulting Impact on Drug Product Formulation [J]. *Pharm Res*, 37(2020) 94.<http://dx.doi.org/10.1007/s11095-020-02813-z>
- [10] X. M. Liao, R. Krishnamurthy, R. Suryanarayanan. Influence of the Active

- Pharmaceutical Ingredient Concentration on the Physical State of Mannitol-Implications in Freeze-Drying [J]. *Pharm Res*, 22(2005) 1978-1985.<http://dx.doi.org/10.1007/s11095-005-7625-x>
- [11] C. Yu, C. Zhang, X. Guan, D. Yuan. The Solid Dispersion of Resveratrol with Enhanced Dissolution and Good System Physical Stability [J]. *J Drug Delivery Sci Technol*, 84(2023).<http://dx.doi.org/10.1016/j.jddst.2023.104507>
- [12] B. S. Alotaibi, M. A. Khan, K. Ullah, H. Yasin, A. Mannan, S. A. Khan, G. Murtaza. Formulation and Characterization of Glipizide Solid Dosage Form with Enhanced Solubility [J]. *PLoS One*, 19(2024).<http://dx.doi.org/10.1371/journal.pone.0297467>
- [13] S. Tambe, D. Jain, S. K. Meruva, G. Rongala, A. Juluri, G. Nihalani, H. K. Mamidi, P. K. Nukala, P. K. Bolla. Recent Advances in Amorphous Solid Dispersions: Preformulation, Formulation Strategies, Technological Advancements and Characterization [J]. *Pharmaceutics*, 14(2022) 2203.<http://dx.doi.org/10.3390/pharmaceutics14102203>
- [14] X. Lu, J. Huang, M. Pinelo, G. Chen, Y. Wan, J. Luo. Modelling and Optimization of Pervaporation Membrane Modules: A Critical Review [J]. *J Membr Sci*, 664(2022).<http://dx.doi.org/10.1016/j.memsci.2022.121084>
- [15] A. Jouyban-Gharamaleki. The Modified Wilson Model and Predicting Drug Solubility in Water-Cosolvent Mixtures [J]. *Chemical & Pharmaceutical Bulletin*, 46(1998) 1058-1061
- [16] M. Sun, J. Cai, R. Shahriari. Activity Coefficient and Co<sub>2</sub> Solubility Studies of Aqueous Alkyl Ammonium Salts Using Electrolyte Pc-Saft Eos [J]. *J Solution Chem*, 51(2022) 1229-1246.<http://dx.doi.org/10.1007/s10953-022-01184-w>
- [17] S. Wang, G. Sadowski, Y. Ji. Strategy of Coupling Artificial Intelligence with Thermodynamic Mechanism for Predicting Complex Polymer Viscosities [J]. *ACS Sustainable Chem Eng*, 12(2024) 4631-4643.<http://dx.doi.org/10.1021/acssuschemeng.3c08185>
- [18] I. Ushiki, A. Miyajima, R. Fujimitsu, S. Takishima. Modeling Cobalt (Iii) Acetylacetonate and Iron (Iii) Acetylacetonate Solubilities in Supercritical Co<sub>2</sub> with Pc-Saft Based on Experimentally-Determined Solid-Liquid Equilibria in Organic Solvents [J]. *J Supercrit Fluids*, 196(2023).<http://dx.doi.org/10.1016/j.supflu.2023.105882>
- [19] S. Dohrn, C. Luebbert, K. Lehmkemper, S. O. Kyeremateng, M. Degenhardt, G. Sadowski. Phase Behavior of Pharmaceutically Relevant Polymer/Solvent Mixtures [J]. *Int J Pharm*, 577(2020) 119065.<http://dx.doi.org/10.1016/j.ijpharm.2020.119065>
- [20] E.-S. Ha, H. Park, S.-K. Lee, J.-S. Jeong, J.-S. Kim, M.-S. Kim. Solubility, Solvent Effect, and Modelling of Oxcarbazepine in Mono-Solvents and N-Methyl-2-Pyrrolidone Plus Water Solvent Mixtures at Different Temperatures and Its Application for the Preparation of Nanosuspensions [J]. *J Mol Liq*, 339(2021) 116792.<http://dx.doi.org/10.1016/j.molliq.2021.116792>
- [21] R. Paus, A. Prudic, Y. Ji. Influence of Excipients on Solubility and Dissolution



- of Pharmaceuticals [J]. *Int J Pharm*, 485(2015) 277-287.<http://dx.doi.org/10.1016/j.ijpharm.2015.03.004>
- [22] D. Wu, Y. Ji. Influence of Polymeric Excipients on the Solubility of Aspirin: Experimental Measurement and Model Prediction [J]. *Fluid Phase Equilib*, 508(2020).<http://dx.doi.org/10.1016/j.fluid.2019.112450>
- [23] Q. Chen, Y. Ji, K. Ge. Influence of Excipients on Thermodynamic Phase Behavior of Pharmaceutical/Solvent Systems: Molecular Thermodynamic Model Prediction [J]. *Chem Eng Sci*, 244(2021).<http://dx.doi.org/10.1016/j.ces.2021.116798>
- [24] J. Gross, G. Sadowski. Perturbed-Chain Saft: An Equation of State Based on a Perturbation Theory for Chain Molecules [J]. *Ind Eng Chem Res*, 40(2001) 1244-1260.<http://dx.doi.org/10.1021/ie0003887>
- [25] Y. H. Ji, R. Paus, A. Prudic, C. Lübbert, G. Sadowski. A Novel Approach for Analyzing the Dissolution Mechanism of Solid Dispersions [J]. *Pharm Res*, 32(2015) 2559-2578.<http://dx.doi.org/10.1007/s11095-015-1644-z>
- [26] J. P. Wolbach, S. I. Sandler. Using Molecular Orbital Calculations to Describe the Phase Behavior of Cross-Associating Mixtures [J]. *Ind Eng Chem Res*, 37(1998) 2917-2928.<http://dx.doi.org/10.1021/ie9707811>
- [27] F. Ruether, G. Sadowski. Modeline the Solubility of Pharmaceuticals in Pure Solvents and Solvent Mixtures for Drug Process Design [J]. *J Pharm Sci*, 98(2009) 4205-4215.<http://dx.doi.org/10.1002/jps.21725>
- [28] J. Tao, Y. Sun, G. G. Z. Zhang, L. Yu. Solubility of Small-Molecule Crystals in Polymers: D-Mannitol in Pvp, Indomethacin in Pvp/Va, and Nifedipine in Pvp/Va [J]. *Pharm Res*, 26(2009) 855-864.<http://dx.doi.org/10.1007/s11095-008-9784-z>
- [29] A. Prudic, Y. H. Ji, G. Sadowski. Thermodynamic Phase Behavior of Api/Polymer Solid Dispersions [J]. *Mol Pharmaceutics*, 11(2014) 2294-2304.<http://dx.doi.org/10.1021/mp400729x>
- [30] S. Miraghapour, M. Pirdashti, S. M. Arzideh, P. Mobalegholeslam, I. Khoiroh. Phase Equilibria of the Ternary System of Lithium Sulfate Plus Polyethylene Glycol (Peg3000) + Water at Different Ph: Experiment Determination, Correlation, and Thermodynamic Modeling [J]. *J Chem Eng Data*, 68(2023) 183-196.<http://dx.doi.org/10.1021/acs.jced.2c00592>
- [31] K. Kothari, V. Ragoonanan, R. Suryanarayanan. The Role of Polymer Concentration on the Molecular Mobility and Physical Stability of Nifedipine Solid Dispersions [J]. *Mol Pharmaceutics*, 12(2015) 1477-1484.<http://dx.doi.org/10.1021/mp500800c>
- [32] K. Mejbri, A. Taieb, A. Bellagi. Phase Equilibria Calculation of Binary and Ternary Mixtures of Associating Fluids Applying Pc-Saft Equation of State [J]. *J Supercrit Fluids*, 104(2015) 132-144.<http://dx.doi.org/10.1016/j.supflu.2015.05.025>
- [33] M. Klajmon. Investigating Various Parametrization Strategies for Pharmaceuticals within the Pc-Saft Equation of State [J]. *J Chem Eng Data*, 65(2020) 5753-5767.<http://dx.doi.org/10.1021/acs.jced.0c00707>

- [34] K. Nam, E. S. Ha, J. S. Kim, D. H. Kuk, D. H. Ha, M. S. Kim, C. W. Cho, S. J. Hwang. Solubility of Oxcarbazepine in Eight Solvents within the Temperature Range  $T = (288.15-308.15)$  K [J]. *J Chem Thermodyn*, 104(2017) 45-49.<http://dx.doi.org/10.1016/j.jct.2016.09.011>
- [35] M. D. Zhang, K. Ge, Y. X. Chen, Y. H. Ji. Solubility Prediction and Dissolution Mechanism Analysis of Etodolac in Complex Polymer Solutions Based on Thermodynamic and Interfacial Mass Transfer Models [J]. *Ind Eng Chem Res*, 63(2023) 731-742.<http://dx.doi.org/10.1021/acs.iecr.3c03638>
- [36] M. Zhang, W. Fan, K. Ge, Y. Ji. Influence of Polymers on Oxaprozin Dissolution Kinetics and Mechanisms [J]. *Chemical Engineering Research & Design*, 200(2023) 803-811.<http://dx.doi.org/10.1016/j.cherd.2023.11.051>
- [37] Q. Chen, Y. H. Ji, K. Ge. Influence of Excipients on Thermodynamic Phase Behavior of Pharmaceutical/Solvent Systems: Molecular Thermodynamic Model Prediction [J]. *Chem Eng Sci*, 244(2021) 116798.<http://dx.doi.org/10.1016/j.ces.2021.116798>
- [38] G. S. Soave, S. Sama, M. I. Oliveras. A New Method for the Prediction of Vle and Thermodynamic Properties. Preliminary Results with Alkane-Ether-Alkanol Systems [J]. *Fluid Phase Equilib*, 156(1999) 35-50.[http://dx.doi.org/10.1016/s0378-3812\(99\)00022-9](http://dx.doi.org/10.1016/s0378-3812(99)00022-9)
- [39] F. Qian, J. Huang, M. A. Hussain. Drug-Polymer Solubility and Miscibility: Stability Consideration and Practical Challenges in Amorphous Solid Dispersion Development [J]. *J Pharm Sci*, 99(2010) 2941-2947.<http://dx.doi.org/10.1002/jps.22074>
- [40] C. S. Liu, K. G. H. Desai, C. G. Liu. Solubility of Rofecoxib in the Presence of Mannitol, Poly(Vinylpyrrolidone) K30, Urea, Polyethylene Glycol 4000, and Polyethylene Glycol 6000 at (298.15, 303.15, and 308.15) K [J]. *J Chem Eng Data*, 50(2005) 661-665.<http://dx.doi.org/10.1021/je049631p>

**Declaration of interests**

The authors declare that they have no known competing financial interests or personal relationships that could have appeared to influence the work reported in this paper.

The authors declare the following financial interests/personal relationships which may be considered as potential competing interests:

Journal Pre-proof